

# AUF1 gene transfer increases exercise performance and improves skeletal muscle deficit in adult mice

Dounia Abbadi,<sup>1</sup> John J. Andrews,<sup>1</sup> Olga Katsara,<sup>1</sup> and Robert J. Schneider<sup>1</sup>

<sup>1</sup>Department of Microbiology, New York University School of Medicine, 550 First Avenue, New York, NY 10016, USA

**Muscle function and mass begin declining in adults long before evidence of sarcopenia and include reduced mitochondrial function, although much remains to be characterized. We found that mRNA decay factor AU-rich mRNA binding factor 1 (AUF1), which stimulates myogenesis, is strongly reduced in skeletal muscle of adult and older mice in the absence of evidence of sarcopenia. Muscle-specific adeno-associated virus (AAV)8-AUF1 gene therapy increased expression of AUF1, muscle function, and mass. AAV8 AUF1 muscle gene transfer in 12-month-old mice increased the levels of activated muscle stem (satellite) cells, increased muscle mass, reduced markers of muscle atrophy, increased markers of mitochondrial content and muscle fiber oxidative capacity, and enhanced exercise performance to levels of 3-month-old mice. With wild-type and AUF1 knockout mice and cultured myoblasts, AUF1 supplementation of muscle fibers was found to increase expression of Peroxisome Proliferator-activated Receptor Gamma Co-activator 1-alpha (PGC1 $\alpha$ ), a major effector of skeletal muscle mitochondrial oxidative metabolism. AUF1 stabilized and increased translation of the *pgc1 $\alpha$*  mRNA, which is strongly reduced in adult muscle in the absence of AUF1 supplementation. Skeletal muscle-specific gene transfer of AUF1 therefore restores muscle mass, increases exercise endurance, and may provide a therapeutic strategy for age-related muscle loss.**

## INTRODUCTION

As we age, we progressively lose muscle mass and strength, which can be a significant source of frailty, increased fractures, and mortality in the elderly population.<sup>1,2</sup> In fact, muscle mass declines by 3%–10% per 10 years after the age of 25.<sup>3</sup> This loss of muscle mass occurs well before the onset of significant loss of muscle that typifies sarcopenia but is evident in loss of strength and function.<sup>4,5</sup> Although regular resistance exercise is the most effective intervention in slowing muscle loss and atrophy with aging,<sup>6</sup> therapeutic strategies also need to be developed to reverse age-related muscle decline. However, there is still an incomplete understanding of molecular targets for therapeutic intervention.

Skeletal muscle stem (satellite) cells are indispensable for muscle regeneration.<sup>7,8</sup> They reside under the basal lamina, between striated muscle fibers (myofibers), which are the contractile cellular bun-

dles.<sup>9,10</sup> Upon physical injury to muscle, the anatomical niche is disrupted, and the normally quiescent but highly polarized satellite cells that are intimately attached to myofibers sense the anatomical disruption, become activated, and divide asymmetrically. Some satellite cells reconstitute the quiescent stem cell population, while others differentiate and fuse to form new myofibers.<sup>11</sup> Myogenic regulatory factors (MRFs) such as MyoD, Myf5, Myogenin, and others are transcription regulatory factors that orchestrate the myogenic fate of satellite cells.<sup>12</sup> Activation of satellite cells requires transcription factor Pax7 with the co-expression of MRFs MyoD and Myf5 to promote satellite cell transient proliferation and differentiation into myogenic progenitor cells known as myoblasts.<sup>13,14</sup> Co-expression of Pax7 and Myf5 therefore specifically identifies activated satellite cells committed to differentiation in the process of orchestrating myogenesis.<sup>7</sup> Both quiescent and activated satellite cells express the Pax7, which is required for both satellite cell maintenance and muscle regeneration potential.<sup>15–17</sup> In adults, the major role of satellite cells is the regeneration of skeletal muscle,<sup>18</sup> which lose the capacity of muscle regeneration with aging and to some extent self-renewal, resulting in loss of function and satellite cell number.<sup>19</sup>

Myofibers are divided into two types that display different contractile and metabolic properties: slow twitch (type I) and fast twitch (type II). Slow- and fast-twitch myofibers are defined according to their contraction speed, metabolism, and type of myosin gene expressed.<sup>10,20</sup> Slow-twitch myofibers are rich in mitochondria, preferentially utilize oxidative metabolism, and provide resistance to fatigue at the expense of speed of contraction. Fast-twitch myofibers are further subdivided into three types, IIa, IIb, and IIx/d, defined by the type of myosin heavy chain (MHC) proteins expressed, which also vary in their contractile properties.<sup>10</sup> Type IIb myofibers are the most glycolytic fibers. They provide rapid contractile response but fatigue rapidly and are typically mitochondria poor. Type IIa and IIx myofibers are predominantly glycolytic but feature more oxidative properties than type IIb and less than type I fibers. Fast-twitch myofibers more readily atrophy in

Received 14 April 2021; accepted 9 July 2021;  
<https://doi.org/10.1016/j.omtm.2021.07.005>.

**Correspondence:** Robert J. Schneider, Department of Microbiology, New York University School of Medicine, 550 First Avenue, New York, NY 10016, USA.

**E-mail:** [robert.schneider@nyumc.org](mailto:robert.schneider@nyumc.org)



response to nutrient deprivation, traumatic damage, advanced age-related loss (sarcopenia), and cancer-mediated cachexia, whereas type I slow-twitch myofibers are more resilient.<sup>21–23</sup> However, although type I slow-twitch myofibers are more resistant to atrophy with aging, they too can decrease in size and number, also reducing muscle mass.<sup>24</sup> Moreover, reduced type I fiber oxidative capacity reflects reduced mitochondrial function, resulting in reduced muscle volume.<sup>25–27</sup> The molecular determinants that maintain type I myofibers are only partially characterized but are known to include sustained mitochondrial function.<sup>5,26,28</sup>

Mitochondrial biogenesis plays a major role in myogenesis, and, accordingly, reduced or dysfunctional mitochondrial activity promotes muscle atrophy with age.<sup>5,26,28</sup> For instance, Peroxisome Proliferator-activated Receptor Gamma Co-activator 1-alpha (PGC1 $\alpha$  or Ppargc1) is a physiological regulator of mitochondrial biogenesis and type I myofiber specification.<sup>29</sup> PGC1 $\alpha$  stimulates mitochondrial biogenesis and oxidative metabolism through increased expression of nuclear respiratory factors (NRFs) such as NRF1 and 2 that stimulate mitochondrial biosynthesis and mitochondria transcription factor A (Tfam) and, in addition to mitochondrial biosynthesis, also promote slow myofiber formation through increased expression of Mef2 proteins.<sup>29–32</sup> Importantly, PGC1 $\alpha$ -mediated mitochondrial biogenesis protects muscle from atrophy due to disuse, certain myopathies, starvation, sarcopenia, cachexia, and other causes.<sup>33–36</sup> Reciprocally, aging muscle demonstrates decreased levels and activity of PGC1 $\alpha$  and increased levels of detrimental reactive oxygen species (ROS), a hallmark of mitochondrial dysfunction.<sup>28</sup>

Skeletal muscle can remodel between slow- and fast-twitch myofibers in response to physiological stimuli, load bearing, atrophy, disease, and injury,<sup>20</sup> involving transcriptional, metabolic, and post-transcriptional control mechanisms.<sup>10,37</sup> The ability to selectively generate or promote a switch to slow-twitch muscle may provide greater resistance to muscle atrophy<sup>24,38</sup> and, as suggested, an effective therapy for sarcopenia, Duchenne muscular dystrophy, cachexia, and other muscle wasting diseases.<sup>39–41</sup>

AU-rich mRNA binding factor 1 (AUF1; HNRNPD) binds with high affinity to repeated AU-rich elements (AREs) located in the 3' untranslated region (3' UTR) found in ~5% of mRNAs. Although AUF1 typically targets ARE-mRNAs for rapid degradation, it can instead stabilize and increase the translation of other ARE-mRNAs, although the mechanism is not as well understood.<sup>42</sup> AUF1 consists of four related protein isoforms identified by their molecular weight (p37, p40, p42, p45), derived by differential splicing of a single pre-mRNA.<sup>42–44</sup> Mutations and/or polymorphisms in AUF1 are linked to human limb girdle muscular dystrophy (LGMD) type 1G,<sup>45</sup> suggesting a critical requirement for AUF1 in post-natal skeletal muscle regeneration and maintenance. In this regard, we previously showed that AUF1 plays a critical role in control of muscle satellite cell fate and muscle regeneration,<sup>27</sup> through programmed rapid degradation of muscle-differentiation checkpoint mRNAs.<sup>45,46</sup>

Here, we report that reduced expression of AUF1 occurs naturally during aging in skeletal muscle in mice, whereas its supplementation by AAV8 AUF1 skeletal muscle gene transfer in adult mice durably and significantly increases skeletal muscle mass, exercise endurance, as well as Pax7<sup>+</sup>-activated satellite cells and myoblasts. AUF1 skeletal muscle gene transfer is shown to increase expression of PGC1 $\alpha$  through stabilization of its mRNA, which is associated with increased mitochondrial biogenesis, and decreases markers of muscle degeneration. AUF1 supplementation of adult and older mice by AAV8 AUF1 gene therapy therefore improves skeletal muscle mass and function by acting on multiple targets of myogenesis and may provide a potential long-term therapeutic intervention for human muscle loss and atrophy.

## RESULTS

### Skeletal muscle AUF1 expression is downregulated in aging adult mice

Because mice deleted in the *auf1* gene undergo an accelerated loss of muscle mass,<sup>45–47</sup> we investigated whether reduced expression of AUF1 with age occurs in wild-type (WT) animals and is involved in age-related muscle decline. We analyzed the expression of AUF1 in limb skeletal muscles of young (3 month) and adult 12- and 18-month-old mice. Compared with 3-month-old young mice, *auf1* mRNA expression was downregulated 3-fold in 12-month-old adults, shown in tibialis anterior (TA) and gastrocnemius muscles, and by one-third in extensor digitorum longus (EDL) and soleus muscles (Figure 1A). In all studies test mRNAs were normalized to *gapdh* or TATA-box binding protein (*tbp*) mRNAs, shown to be unchanged with age in muscle in mice,<sup>48,49</sup> which were also unchanged in abundance regardless of AUF1 expression.<sup>48,49</sup> As shown in the TA muscle, AUF1 protein levels and mRNA levels were similarly changed, reduced ~3-fold at 12 months and 4-fold at 18 months, normalized to muscle total protein and invariant GAPDH (Figure 1B). Reduced skeletal muscle expression of AUF1 in adult mice tracked with reduced muscle mass in limb muscles, shown in the TA, EDL, gastrocnemius, and soleus muscles in 12- and 18-month-old mice compared with 3-month-old animals (Figure S1A). Importantly, by 18 months of age, loss of muscle mass largely plateaued from 12-month values, which accords with other studies.<sup>5,28,50</sup> The TA muscle was reduced in relative mass by almost 50%, the EDL by 30%, the soleus by almost 50%, and the gastrocnemius by 25%. It should be noted that there was also reduced absolute muscle mass at 12 and 18 months that cannot be accounted for by an increase in overall body weight in adults compared with young mice (Table 1). In 12- and 18-month-old mice, the gastrocnemius was reduced by 11% and 14% and the TA muscle by 18% and 24%, respectively, which has been observed by others as well.<sup>26,28</sup>

### AUF1 skeletal muscle gene transfer enhances exercise endurance of 12- and 18-month-old adult mice

We determined whether loss of skeletal muscle mass with age in mice is a result of reduced expression of AUF1 in skeletal muscle. We developed an adeno-associated virus type 8 (AAV8) vector to deliver and selectively express AUF1 in skeletal muscle. AAV vectors express

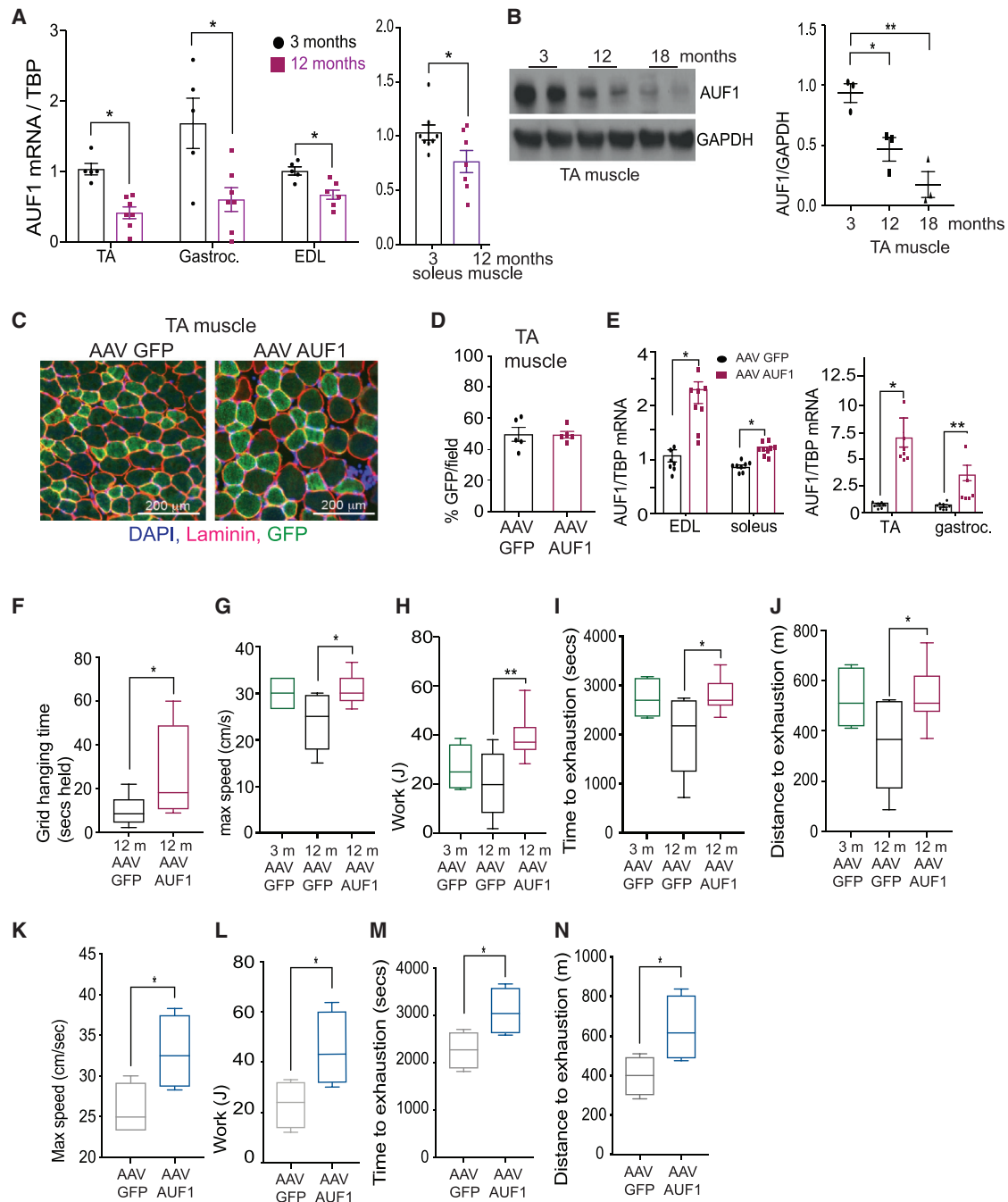


**Figure 1. AUF1 supplementation in skeletal muscle improves exercise endurance in 12- and 18-month-old mice**

(A) Relative expression of *auf1* mRNA in the TA, gastrocnemius, EDL, and soleus muscles normalized to invariant *tbp* mRNA at 3 and 12 months of age in wild-type (WT) mice. (B) Representative immunoblot and quantification of AUF1 protein levels in the TA muscle of WT mice at 3, 12, and 18 months. GAPDH is a loading control.  $n = 2$  mice chosen at random per group. (C) Representative staining of AAV GFP control and AAV AUF1/GFP<sup>+</sup> myofibers in TA muscle 40 days post-administration. (D) Quantification of GFP<sup>+</sup> myofibers in TA muscle 40 days post-AAV administration.  $n = 5$  mice. (E) Relative fold increased expression of *auf1* mRNA in gastrocnemius, TA, EDL, and soleus muscles 40 days post-AAV administration.  $n = 8$  or 9 mice. (F–J) Strength and exercise endurance in 3- and 12-month-old mice 40 days post-AAV administration: (F) grid hanging time, (G) maximum speed, (H) work performance, (I) time to exhaustion, (J) distance to exhaustion.  $n = 5$ –9 mice. (K–N) Strength and exercise endurance 6 months post-AAV administration in 18-month-old mice: (K) maximum speed, (L) work performance, (M) time to exhaustion, (N) distance to exhaustion.  $n = 4$  mice. Mean  $\pm$  SEM from 5 or more independent studies. \* $p < 0.05$ , \*\* $p < 0.01$  by unpaired Mann-Whitney U test.

**Table 1. Mean limb muscle weight with age**

Age	Muscle	Mean weight (mg)	p value
3 month	TA	81.4	
	EDL	18.5	
	soleus	13.7	
	gastroc.	234.5	
12 month	TA	66.5	0.0002
	EDL	17.8	0.65 ns
	soleus	13.7	0.94 ns
	gastroc.	202.4	0.004
18 month	TA	61.8	0.05*
	EDL	17.1	0.44 ns
	soleus	10.9	0.22 ns
	gastroc.	208.2	0.25 ns

\*ns, not significant, unpaired Mann-Whitney U test

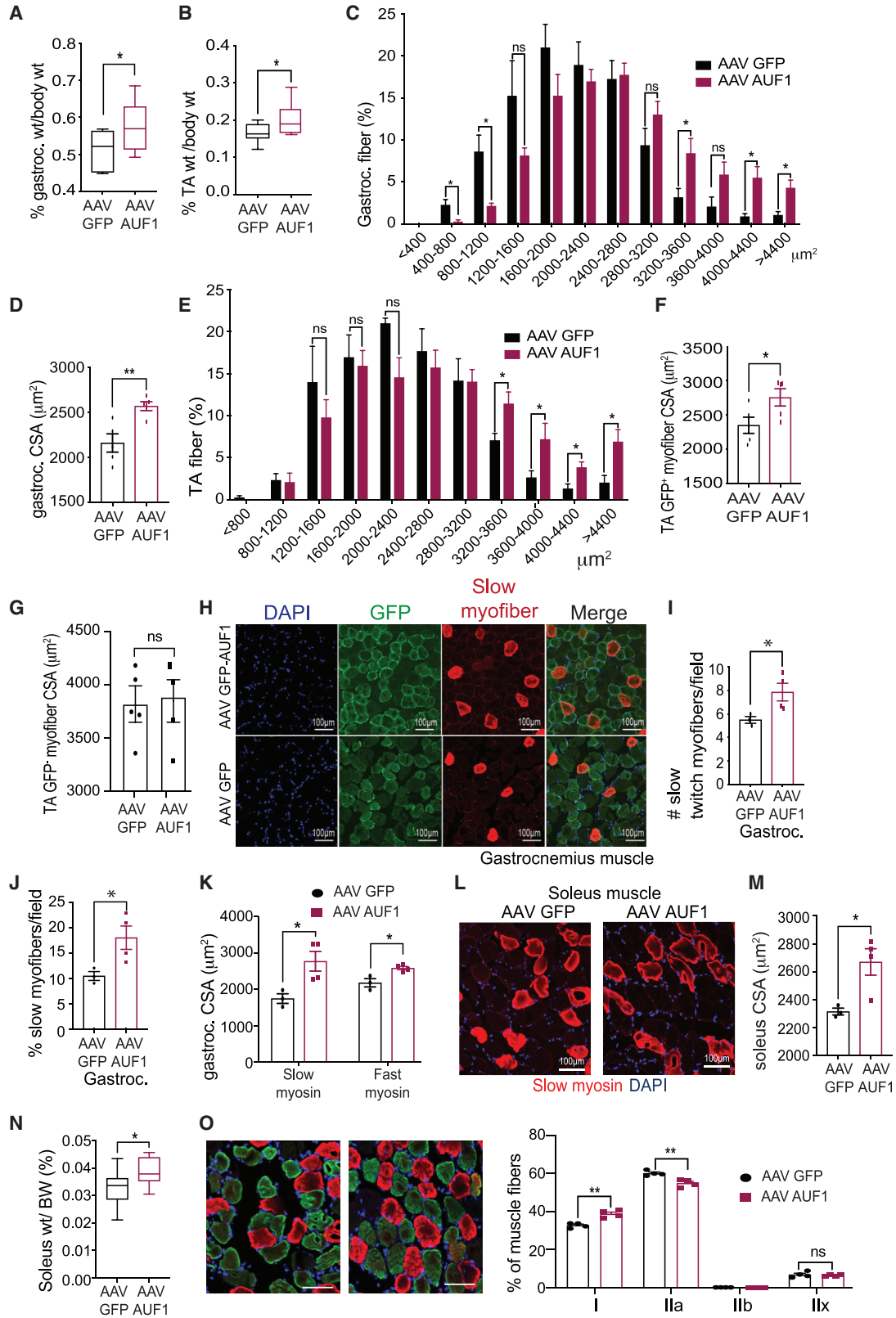
AUF1 and GFP (AUF1-GFP), with GFP translated from the same mRNA as AUF1 directed by the hepatitis C virus (HCV) internal ribosome entry site (IRES) or as a control only GFP. Expression of both genes is controlled by the creatine kinase tMCK promoter that is selectively active in skeletal muscle cells including myoblasts but not detectably active in cardiac muscle cells.<sup>51</sup> Mice aged 3 and 12 months were administered a single retro-orbital injection of either AAV AUF1-GFP or control AAV GFP vectors ( $2.5 \times 10^{11}$  viral genome copies). When analyzed starting at 40 days post-administration of AAV vectors, as shown in 12-month-old mice, both AAV AUF1-GFP and AAV GFP control vector-treated animals displayed similar vector transduction and retention rates, shown by TA muscle GFP staining (Figures 1C and 1D). *auf1* mRNA expression in skeletal muscle was increased by AAV8 AUF1-GFP administration, on average 2.5-fold in EDL, 6-fold in TA, 2.5-fold in gastrocnemius, and slightly in soleus muscle (Figure 1E). AUF1 protein levels in gene-transferred animals in skeletal muscle, as shown in the TA muscle, demonstrated 4- to 6-fold increased expression over endogenous levels, corresponding to *auf1* mRNA levels (Figure 1E; Figure S1B). Representative immunofluorescence staining also demonstrated strong uptake and expression of AUF1 localized in nuclei (Figure S1C, white arrows) and sarcoplasm (Figure S1C, yellow arrows) as expected in AAV AUF1-GFP-infected TA muscle fibers that is not seen for control AAV GFP. There was no evidence for increased expression of AUF1 in non-muscle tissues compared with control mice administered either vector (kidney, lung, spleen, liver) (Figure S1D), demonstrating strong tissue specificity for skeletal muscle expression controlled by the tMCK promoter, as shown by others.<sup>51</sup> Importantly, Pax7 expression, a key marker for activation of muscle satellite cells and proliferating myoblasts, was also increased 3- to 4-fold with AAV AUF1-GFP administration (Figure S1E). Moreover, increased expression of Pax7 was limited to cells expressing AUF1-GFP, which was not evident in cells expressing only GFP in the absence of AUF1 gene delivery (Figure S1F). Correspondingly, markers of muscle atrophy such as *trim63* and *fbxo32*<sup>24</sup>, were down-

regulated 2- to 3-fold in the TA muscle and 0.5- to 4-fold (respectively) in gastrocnemius muscle in animals administered AAV AUF1-GFP but not AAV GFP (Figures S1G and S1H). These data indicate that AUF1 gene transfer into skeletal muscle is sufficient to reduce markers of muscle atrophy coincident with activation of satellite cells and myoblasts.

We therefore investigated whether AUF1 gene transfer can increase physical endurance in 12- and 18-month-old mice, using a number of well-established criteria. Twelve-month-old mice were administered AAV8 AUF1-GFP or control AAV8 GFP and then tested at 40 days post-administration. AUF1-supplemented mice showed an ~50% improvement in grid hanging time (Figure 1F), a measure of limb girdle skeletal muscle strength and endurance. When tested by more stringent treadmill criteria, AAV AUF1-GFP mice displayed 25% higher maximum speed (Figure 1G) and 50% increase in work performance (Figure 1H) compared with AAV GFP control mice, as well as 25% greater time to exhaustion and 30% increased distance to exhaustion (Figures 1I and 1J). Compared with 3-month-old mice receiving control AAV GFP, 12-month-old mice receiving AUF1 supplementation gained physical endurance capacity equivalent to the level of 3-month-old mice. Physical endurance was also tested 6 months post-AAV-AUF1 supplementation in 12-month-old mice that were 18 months old at the time of testing. Maximum speed (Figure 1K), work performed (Figure 1L), as well as time and distance to exhaustion (Figures 1M and 1N) were all significantly higher in AUF1-AAV-treated animals, demonstrating durable and significantly increased levels of physical endurance, similar to 12-month-old mice at 40 days post-supplementation AUF1 supplementation. These results demonstrate that supplementation with AUF1 is durable at 6 months post-treatment. We therefore investigated the biological and molecular characteristics of AUF1-supplemented skeletal muscle.

#### **AUF1 gene therapy increases muscle mass, slow-twitch and fast-twitch myofibers, and mitochondrial oxidative potential**

Skeletal muscles vary in slow-twitch (type I) and fast-twitch (type II) myofibers. In the mouse, different techniques yield fairly consistent compositions but with some ambiguity related to the large presence of intermediate hybrid fibers ranging up to 15%–20% of skeletal muscle in the adult mouse.<sup>52–54</sup> EDL and gastrocnemius muscles are composed largely of type II fast-twitch myofibers (90%–95% fast, 5%–10% slow), the TA is ~20% type I and 80% type II, whereas the mouse soleus muscle is highly enriched in type I slow-twitch myofibers (nearly 40% slow, 60% fast).<sup>10,52,53,55</sup> Analysis of the gastrocnemius and TA muscles showed that 12-month-old adult mice administered AAV AUF1-GFP compared with AAV GFP controls gained an average increase of ~20% in muscle mass relative to body weight by 40 days (Figures 2A and 2B). In 12-month-old mice, AUF1-supplemented gastrocnemius and TA muscles increased in muscle fiber size (myofiber cross-sectional area, CSA), particularly in the percentage of larger myofibers (>3,200  $\mu\text{m}^2$ ), as well as number, which largely represents increased fast-twitch type II fibers in mice (Figures 2C–2F). Notably, increased myofiber size can be indicative of increased muscle hypertrophy, which if sarcoplasmic is



(legend on next page)

associated with increased strength.<sup>56,57</sup> In contrast to AUF1-transduced myofibers, non-transduced (GFP<sup>-</sup>) myofibers saw no increase in CSA, as shown for the TA muscle in animals administered either AAV GFP or AAV AUF1-GFP (Figure 2G). Non-transduced myofibers tended to have a greater CSA than vector-transduced fibers expressing GFP. It is possible that the largest fibers are not efficiently infected. It is known that AAV6 preferentially infects smaller CSA myofibers, whereas AAV9 shows no preference,<sup>58</sup> which has not been studied for AAV8.

We also analyzed the gastrocnemius muscle in animals administered either control GFP or AUF1-GFP AAV8, by co-staining for GFP and slow myosin to determine AAV8 infection levels in slow- and fast-twitch myofibers (Figure 2H). The AAV8 vector efficiently infected both slow myofibers (red and GFP stained) and fast myofibers (GFP stained only). Since type I myofibers comprise a small percentage of most muscles, we also investigated the effect of supplemental AUF1 expression specifically on slow myofibers by co-staining with slow myosin and GFP. In the gastrocnemius muscle, AUF1 supplementation increased by >50% the number of type I myofibers per field, the percentage per field, and the CSA (Figures 2H–2K). In the soleus muscle, which is composed of ~40% type I fibers, the CSA was similarly increased with AUF1 supplementation, as was muscle weight normalized to body weight (Figures 2L–2N). Next, we carried out immunostaining of the different myofibers in the soleus muscle at 40 days post-AUF1 gene transfer in 12-month-old mice (Figure 2O). These data show that AUF1 gene transfer results in a small increase in type I fibers and a small reduction in type IIa myofibers in the soleus muscle, without altering levels of IIb and IIx myofibers. These data correlate with increased endurance in mice receiving AUF1 gene transfer and that AUF1 promotes formation of type I myofibers, by myofiber regeneration and possibly conversion and possibly conversion. Therefore, we carried out immunostaining of Pax7 and Myf5 in the TA muscle of 12-month-old mice 40 days after AUF1 gene transfer to determine levels of satellite cell activation indicative of muscle hypertrophy and regeneration. As shown in representative images (Figure S11), Myf5 staining correlated with Pax7 co-staining, supporting the conclusion that AUF1 gene therapy promotes muscle hypertrophy, regeneration, and fiber conversion.

Expression levels of different myosin type mRNAs also support that AUF1 gene transfer resulted in real gain in skeletal muscle mass. The major slow-twitch myosin mRNA, *myh7*, was increased 6-fold

in gastrocnemius and 2-fold in soleus muscle with AUF1 gene transfer (Figures 3A and 3B). Fast myosin mRNAs such as *myh1*, *myh2*, and *myh4* were not statistically changed (Figures 3C and 3D).

Increased expression levels for several genes are indicative of increased myofiber hypertrophy, oxidative processes, and mitochondrial biogenesis. Slow-twitch myofibers in particular are enriched in oxidative mitochondria.<sup>10</sup> We focused on the gastrocnemius muscle because it demonstrated a median response to AUF1 gene therapy and it is not biased toward enrichment of slow-twitch myofibers. Although AUF1 gene transfer had no effect on gastrocnemius mRNA levels encoded by non-mitochondrial genes such as *ppara* (peroxisome proliferator-activated receptor alpha) or *six1* (Sineoculis homeobox homolog 1), it increased the level of mitochondrial mRNAs by 4-fold for *tfam* (mitochondria transcription factor A), by 6-fold for *acadvl* (acyl-CoA dehydrogenase very long chain), and by 2- to 3-fold for *nrf1* and *nrf2* (nuclear respiratory factors 1 and 2) (Figures 3E–3H). The ratio of mitochondrial to nuclear DNA also increased in the gastrocnemius with AUF1 gene transfer, indicative of increased mitochondrial content at both 40 days and 6 months post-gene transfer (Figures 3I and 3J). Finally, we quantified the activity of myofiber succinate dehydrogenase (SDH), a mitochondrial membrane protein complex in muscle that is an established indicator of mitochondrial activity and oxidative potential.<sup>59</sup> Immunohistochemical determination of SDH activity showed that it was strongly increased in TA, gastrocnemius, and EDL muscle fibers, and only in animals receiving AAV AUF1 supplementation (Figure 3K), averaging 30% or more in all three muscles (Figure 3L). Collectively, these results show that AUF1 promotes transition from fast- to slow-twitch myofiber.

#### AUF1 stimulates slow-twitch muscle phenotype in part by stabilizing the *pgc1α* ARE-mRNA and increasing PGC1 $\alpha$ expression

A key feature of slow muscle is that it confers exercise endurance because slow-twitch myofibers have higher oxidative capacity than fast-twitch fibers.<sup>60,61</sup> We therefore characterized the level of AUF1 expression in different muscles with varying proportions of slow and fast myofibers. There was a 2- to 4-fold higher level of expression of *auf1* mRNA and AUF1 protein in the soleus muscle of 3- and 12-month-old untreated mice compared to other muscle types with fewer slow-twitch myofibers (Figures 4A–4C). Accordingly, of the lower limb skeletal muscles, the soleus muscle is the most enduring

#### Figure 2. AUF1 gene transfer increases muscle mass, myofiber CSA, and number

(A and B) Muscle weight relative to total body weight 40 days post-AAV administration for gastrocnemius and TA muscles, respectively. n = 8 or 9 mice. (C and D) Frequency distribution of gastrocnemius myofiber CSA and mean area at 40 days post-AAV administration. n = 5 mice/group. (E and F) Frequency distribution of TA muscle CSA and mean area at 40 days post-AAV administration for GFP<sup>+</sup> myofibers. n = 5 mice. (G) TA muscle CSA at 40 days post-AAV administration for GFP<sup>-</sup> myofibers. n = 5 mice. (H) Representative immunostain of slow myofiber (red), GFP (green), and nuclei (DAPI, blue) in gastrocnemius muscle at 40 days post-therapy. (I–K) Slow myofibers per field, percent slow myofibers per field, and mean CSA, respectively, of slow and fast myofibers in gastrocnemius muscle at 40 days post-AAV administration. (L) Representative immunostain of slow myofiber (red) and nuclei (blue) in soleus muscle 40 days after AAV AUF1-GFP or AAV GFP administration. (M) Mean cross surface area (CSA) of slow-twitch soleus muscle myofiber 40 days after AAV AUF1 or AAV GFP administration. n = 3 mice per group. (N) Mean soleus weight in GFP control and AUF1-GFP AAV8-treated animals 40 days post-gene transfer. n = 4 mice per group. (O) Representative immunostaining and quantification of different myofibers in the soleus muscle 6 months post-AUF1 gene transfer in 12-month-old mice. Scale bars, 100  $\mu$ m. Mean shown from 3 or more independent studies. \* p < 0.05, \*\* p < 0.01 by unpaired Mann-Whitney U test.

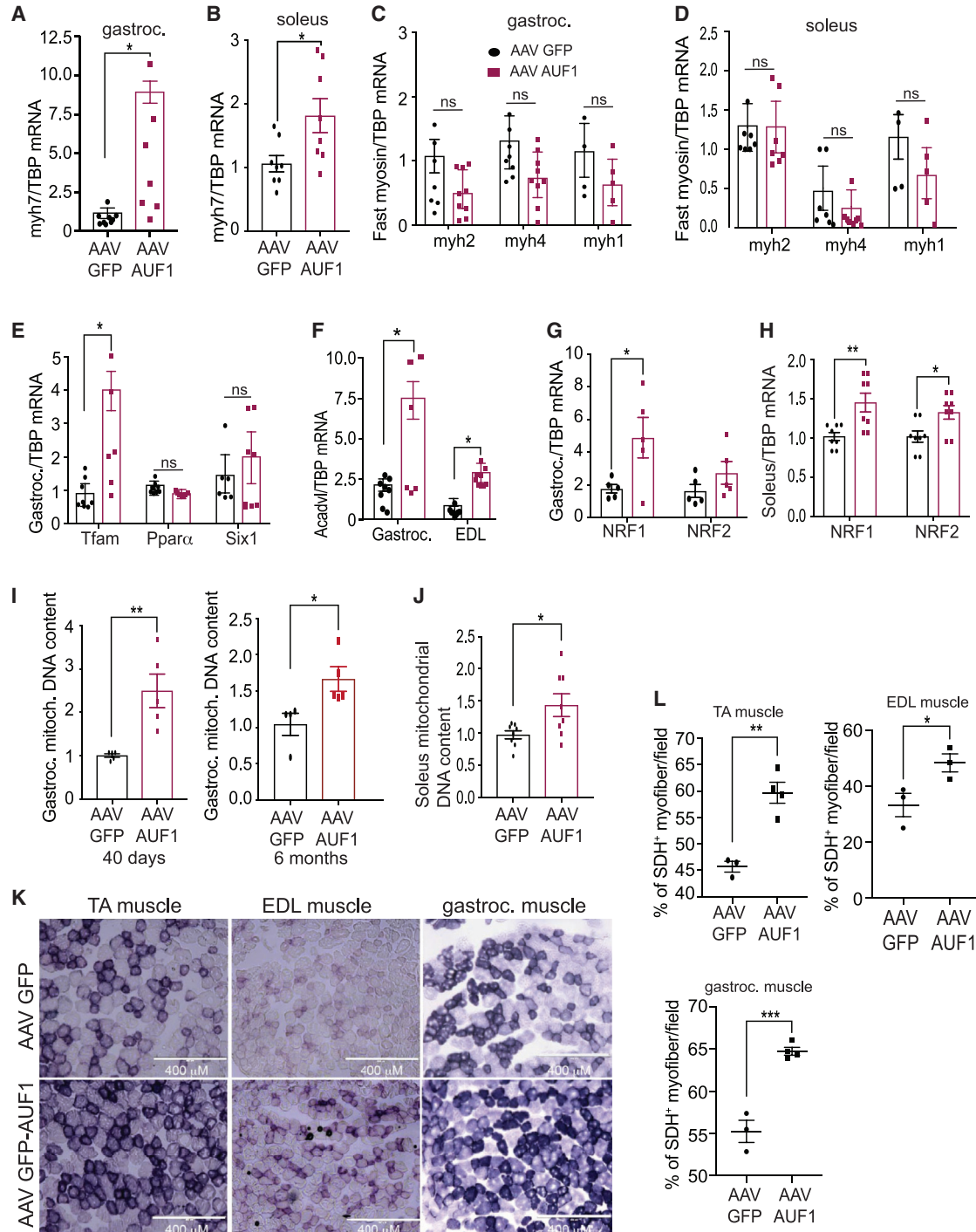


**Figure 3. Molecular markers of skeletal muscle myogenesis in AAV8 AUF1-GFP gene-transferred mice**

(A and B) Relative *myh7* mRNA levels in (A) gastrocnemius and (B) soleus muscles normalized to invariant nuclear TATA-box binding protein (*tbp*) mRNA at 40 days post-gene transfer. (C and D) Relative fast myosin mRNA levels in (C) gastrocnemius and (D) soleus muscles normalized to *tbp* mRNA at 40 days post-gene transfer. (E) Expression levels of non-mitochondrial mRNAs (*pparg*, *six1*) and mitochondrial mRNA in gastrocnemius muscle at 40 days post-gene transfer. (F) Level of mitochondrial mRNA for *acadvl* and *tfam* in gastrocnemius and EDL muscles at 40 days post-gene transfer. (G and H) *nrf1* and *nrf2* mRNA levels in gastrocnemius muscle 40 days post-gene transfer. (I and J)

(legend continued on next page)

and the most enriched in slow-twitch myofibers<sup>10,53</sup> and expresses much higher levels of *myh7* (Figure 4D), the main slow-twitch myofiber myosin. We therefore assessed the role of AUF1 in expression of different levels of myosin mRNAs by deletion of AUF1 in C2C12 mouse myoblasts. Deletion of AUF1 increased the expression of fast-twitch *myh2* mRNA levels, whereas slow myosin mRNAs, such as *myh7* or *myl2*, were decreased (Figure S2A), consistent with greater specification of slow-twitch myofiber development by AUF1. Myocyte enhancer factor 2 (MEF2C) is a transcriptional regulator of overall skeletal muscle development that can activate or repress different myogenic transcriptional programs.<sup>62–64</sup> Its increased expression is also consistent with increased generation of type I slow-twitch muscle. We examined MEF2C levels because AUF1 was previously shown to promote *mef2c* ARE-mRNA translation without altering its mRNA stability.<sup>29,65</sup> *mef2c* mRNA levels were not increased at 40 days post-AUF1 supplementation and showed only a slight increase at 6 months (Figures S2B and S2C). MEF2C protein levels were moderately increased at 40 days post-supplementation (Figure S2D), whereas PGC1 $\alpha$  protein levels were increased strongly at 40 days post-supplementation. As shown later (Figure 4G), increased PGC1 $\alpha$  protein levels were sustained at 6 months post-AUF1 supplementation.

Although the PGC1 $\alpha$  protein can stimulate expression of *mef2c* mRNA, it is PGC1 $\alpha$  that drives the specification and development of slow-twitch myofibers.<sup>29</sup> Like the *mef2c* mRNA, the *pgc1 $\alpha$*  mRNA also contains an ARE-3' UTR<sup>30</sup> that might be a target for AUF1 regulation. Deletion of the *auf1* gene in C2C12 myoblasts that were induced to differentiate to myotubes, decreased *pgc1 $\alpha$*  mRNA levels by half and protein levels by 4-fold (Figure 4E), suggesting that AUF1 acts to increase PGC1 $\alpha$  protein and mRNA expression. Accordingly, AAV8-AUF1 gene transfer in mice showed that *pgc1 $\alpha$*  mRNA levels were increased 2- to 3-fold in the gastrocnemius and EDL muscles and trended toward upregulation in the TA muscle in 12-month-old mice (Figure 4F). AUF1 gene transfer in 18-month-old mice 6 months post-gene transfer (24 month old mice) also increased *pgc1 $\alpha$*  mRNA levels ~2.5-fold, as shown in the gastrocnemius muscle (Figure 4F), which corresponded to an average 5-fold increase in PGC1 $\alpha$  protein levels (Figure 4G).

We therefore immunoprecipitated AUF1 from WT C2C12 myoblasts 48 h after their differentiation when AUF1 is expressed, with control immunoglobulin G (IgG) or anti-AUF1 antibodies, followed by qRT-PCR to quantify the levels of bound *pgc1 $\alpha$*  mRNA (Figure 4H). AUF1 bound strongly to the *pgc1 $\alpha$*  mRNA in differentiating C2C12 cells. The effect of AUF1 expression on the *pgc1 $\alpha$*  mRNA half-life was determined with WT and AUF1 knockout (KO) C2C12 cells by addition of actinomycin D to block new transcription (Figure 4I). In the absence of AUF1, *pgc1 $\alpha$*  mRNA was reduced almost 3-fold in stability. Studies next determined whether AUF1 acts on the *pgc1 $\alpha$*  3' UTR

AU-rich elements. We inserted the *pgc1 $\alpha$*  3' UTR AU-rich region into the 3' UTR of a luciferase reporter (Figure S2E) and compared control luciferase activity and mRNA levels to luciferase with the *pgc1 $\alpha$*  ARE in transfected C2C12 myoblasts or myoblasts stably transfected with p40 AUF1 to increase AUF1 expression.<sup>46</sup> Three-fold increased expression of AUF1 increased activity (expression) of luciferase by ~3-fold from the mRNA containing the *pgc1 $\alpha$*  AREs and luc-ARE mRNA levels by 6-fold (Figures 4J and 4K). The *pgc1 $\alpha$*  mRNA therefore belongs to the class of ARE-mRNAs that are stabilized rather than destabilized by AUF1, accounting in part for increased levels of PGC1 $\alpha$  protein and increased specification of slow-twitch fiber formation by AUF1. We therefore investigated the effect of AUF1 expression specifically on slow-twitch muscle loss and atrophy.

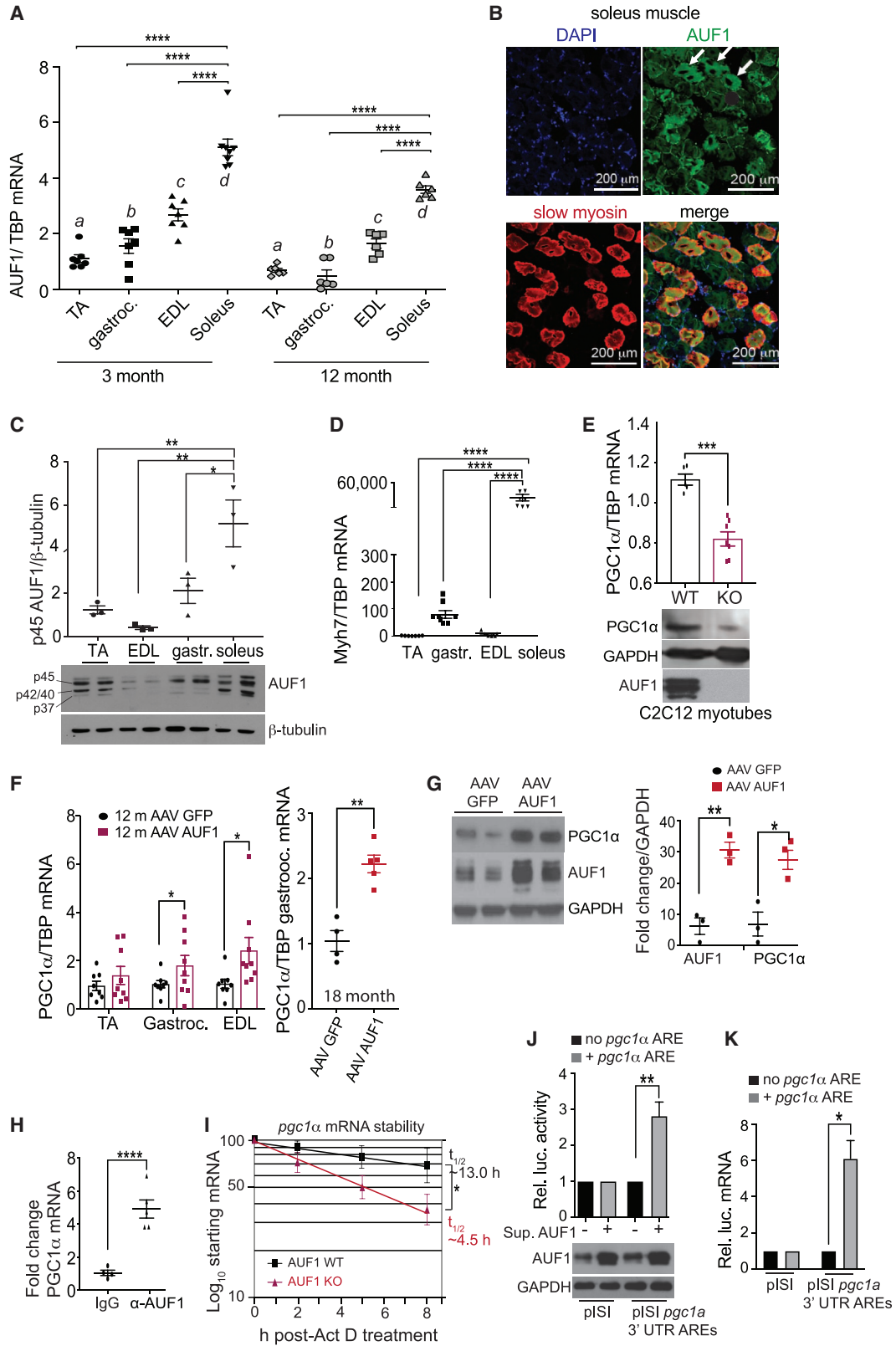
### Loss of AUF1 expression accelerates atrophy of slow-twitch muscle in young mice

To better understand the role of AUF1 gene transfer in the formation and maintenance of slow-twitch myofibers, we investigated slow-twitch myofibers in WT and germline AUF1 KO mice at 3 months of age, before the onset of muscle atrophy that occurs in KO mice.<sup>45</sup> At 3 months, WT and *auf1* KO mice have similar body weights (Figure 5A). Although deletion of *auf1* did not change the size, color (mitochondrial density, myoglobin content), or weight of the TA, EDL, or gastrocnemius muscles, it did reduce the size and weight of the soleus muscle by half at 3 months, which was much paler, indicative of loss of mitochondrial and myoglobin-rich type I myofibers (Figure 5B; Figure S3A). The proportion and number per field of slow myosin myofibers in the AUF1 KO mouse soleus muscle were reduced 40%–50% (Figures 5C–5E; Figure S3B). In contrast, both the proportion and number of fast myosin-expressing myofibers was increased by 25% or more in the absence of AUF1 expression (Figures 5C, 5F, and 5G; Figure S3B). Reduced expression of slow myosin was also seen in the gastrocnemius muscle with *auf1* deletion in *auf1* KO mice (Figures S3C–S3E). In addition, the mean CSA was reduced by 2-fold in slow-twitch myofibers of AUF1 KO mice, as shown in the soleus and gastrocnemius muscles, but was unchanged in fast-twitch myofibers (Figure 5H; Figure S3F). Consistent with these data, AUF1 KO mice at 3 months expressed 3- to 4-fold lower levels of PGC1 $\alpha$  protein than WT mice, as shown in the gastrocnemius and soleus muscles (Figure S3G). AUF1 therefore specifies myogenesis and maintenance of slow-twitch muscle in part by stabilizing the *pgc1 $\alpha$*  mRNA.

### Reduced expression of AUF1 in adult mice accelerates atrophy and decline of both slow- and fast-twitch muscle

At 6 months of age, *auf1* KO mice show a 20% loss of body weight, which is in part a result of loss of skeletal muscle mass (Figures 6A and 6B). Unlike 3-month-old AUF1 KO mice, where the slow-twitch myofiber-rich soleus muscle was the only muscle showing significant

DNA mitochondrial content in gastrocnemius and soleus muscles, respectively, 40 days or 6 months post-gene transfer. Red histogram, AAV AUF1-GFP. Black histogram, AAV GFP. (K) Representative images of succinate dehydrogenase (SDH) enzyme activity in TA, EDL, and gastrocnemius muscles from mice 40 days post-administration of AAV8 GFP or AAV8 AUF1-GFP. (L) Quantitation of SDH-positive myofibers per field for TA, EDL, and gastrocnemius muscles corresponding to (K). n = 3 mice per muscle, 5 fields chosen at random. Mean  $\pm$  SEM from 3 or more independent studies. \*p < 0.05, \*\*p < 0.01, \*\*\*p < 0.001 by unpaired Mann-Whitney U test.



(legend on next page)

atrophy in the absence of AUF1 expression, in 6-month-old mice muscles enriched in fast-twitch or slow-twitch muscles both demonstrate significant atrophy. For instance, the size and weight of the TA, EDL, and gastrocnemius muscles were reduced by ~25% in *auf1* KO compared with WT animals, and the soleus muscle was reduced by almost 50% (Figure 6B). In addition, *auf1* KO mouse skeletal muscles were paler than those of control WT mice, consistent with greater loss of mitochondrial-dense, slow-twitch myofibers (Figure 6C). Accordingly, the mean CSA of both slow- and fast-twitch myofibers, as shown in the soleus and gastrocnemius muscles, showed a striking reduction at 6 months in *auf1* KO mice compared with WT, indicative of overall myofiber atrophy (Figures 6D and 6E). As seen in 3-month-old mice, AUF1 deficiency reduced by half the percentage and number of slow-twitch myofibers per field in the soleus and gastrocnemius muscles (Figures 6F–6I). Thus, although AUF1 specifies development of slow-twitch muscle, its other myogenesis activities as previously described<sup>45,46,65</sup> are essential for maintenance of both slow- and fast-twitch muscle, consistent with the ability of AUF1 gene transfer to promote increased overall muscle mass and function in adult animals.

## DISCUSSION

This work reports four important sets of findings: (1) AUF1 expression in skeletal muscle is diminished in adult compared with young mice, which contributes to a reduction in muscle mass and function; (2) AUF1 gene transfer might provide a therapeutic intervention to delay or possibly reverse the loss of muscle mass and strength with age; (3) AUF1 is required for the maintenance of both slow and fast myofibers; and (4) AUF1 promotes a transition from fast to slow muscle phenotype by increasing PGC1 $\alpha$  levels through stabilization of its mRNA. AUF1 generally promotes rapid decay of ARE-containing mRNAs but can stabilize a subset of other ARE-mRNAs.<sup>42</sup> We previously showed that AUF1 regulates satellite cell maintenance and differentiation in part by reprogramming each stage of myogenesis through selective degradation of short-lived myogenic checkpoint and myogenesis ARE-mRNAs.<sup>45,46</sup> In addition, as shown here, by increasing AUF1 expression levels in skeletal muscles in mice by AAV gene transfer, AUF1 increases the expression of slow myosins and oxidative mitochondrial genes that mediate slow myofiber formation and oxidative phenotype. There is also evidence for reduced AUF1 expression in human skeletal muscle with aging,<sup>66</sup>

although the general inability to obtain serial age-related but otherwise normal muscle specimens limits the ability to expand this finding.

Gene transfer of skeletal muscle with AUF1 by AAV8 gene delivery significantly promoted muscle mass and exercise endurance in 12- and 18-month-old adult mice that had evidence of reduced muscle mass and increased muscle decline and atrophy compared with 3-month-old young mice. Notably, in a rat model designed to characterize skeletal muscle markers of increased physical exercise endurance, two major factors that were found to be increased in expression were AUF1 and PGC1 $\alpha$ .<sup>30</sup> Moreover, an exercise study in mice found that whereas 1 week of exercise induced increased levels of PGC1 $\alpha$ , after 4 weeks of exercise AUF1 increased by as much as 50% without changes in other ARE-binding proteins.<sup>67</sup> Interestingly, *pgc1 $\alpha$* , *tfam*, and *nrf2* mRNAs all contain AREs in their 3' UTRs, which are subject to regulation by ARE-binding proteins, including AUF1.<sup>68</sup> These findings, when combined with our results, suggest that AUF1 programs a feedforward mechanism to promote muscle regeneration through stabilization of *pgc1 $\alpha$*  mRNA and, as we have previously shown, through other AUF1 activities as well.<sup>45,46</sup> Consistent with this conclusion, at a young age AUF1 KO mice demonstrate a reduction of slow-twitch myofiber size and a decreased level of PGC1 $\alpha$  expression.

That AUF1 muscle supplementation increases PGC1 $\alpha$  protein levels suggests an important additional level of AUF1 activity in promoting myogenesis. PGC1 $\alpha$  activates expression of downstream factors such as NRFs and Tfam that promote mitochondrial biogenesis, which is essential for the formation of slow-twitch muscle fibers, reduced fatigability of muscle, and greater oxidative metabolism.<sup>29</sup> These findings, along with enhanced mitochondrial DNA content observed with AUF1 supplementation, suggest that AUF1 is responsible for key activities in slow-twitch myofiber maintenance and increased exercise endurance in mice. Previous studies have shown the benefit of increased PGC1 $\alpha$  expression in muscle damage repair and angiogenesis.<sup>33–36,69,70</sup>

AUF1 skeletal muscle gene transfer is therefore beneficial in countering muscle loss and atrophy because it is required to enable multiple key steps in myogenesis. AUF1 stimulates greater muscle development and physical exercise capacity in aging muscle, which

### Figure 4. AUF1 promotes slow-twitch fiber myogenesis by stabilizing the *pgc1 $\alpha$* mRNA

(A) Relative *auf1* mRNA expression in 3- and 12-month-old WT mice in TA, gastrocnemius, EDL, and soleus muscles. n = 5–7 mice. (B) Representative immunofluorescence staining of AUF1 expression in slow myofibers in 3-month-old mice. (C) Representative immunoblot of AUF1 protein level and quantification in TA, gastrocnemius, EDL, and soleus muscle in 3-month-old mice. (D) Relative *myh7* mRNA expression in 3-month-old mouse TA, gastrocnemius, EDL, and soleus muscles. (E) Relative *pgc1 $\alpha$*  mRNA expression and protein levels in WT C2C12 myoblasts and AUF1 KO myoblasts. (F) Relative *pgc1 $\alpha$*  mRNA expression in TA, gastrocnemius, and EDL muscles 40 days post-treatment and in gastrocnemius at 6 months post-gene transfer in 12-month-old mice. (G) Representative immunoblot of two AAV8-GFP control and AAV8-AUF1 GFP animals (left) and quantification of AUF1 and PGC1 $\alpha$  in three animals per group (right) at 6 months after treatment in 12-month-old mice. (H) *Pgc1 $\alpha$*  mRNA immunoprecipitation with endogenous AUF1 protein in myoblasts 48 h after myotube induction of differentiation in WT C2C12 cells. n = 5. (I) *pgc1 $\alpha$*  mRNA decay rate in WT and AUF1 KO C2C12 cells. (J and K) C2C12 and C2C12 cells overexpressing AUF1<sup>46</sup> were transfected with plasmids expressing luciferase reporters without (pLS1) and with (pLS1 *pgc1 $\alpha$*  3' UTR) the *pgc1 $\alpha$*  3' UTR AREs. Cells were harvested at 36 h, equal protein amounts analyzed by immunoblot, luciferase activity determined, and luciferase mRNA levels quantified. Mean  $\pm$  SEM from 3 or more independent studies. (A and B) \*\*\*\*p < 0.001 by Kruskal-Wallis test. All other panels by unpaired Mann-Whitney U test, \*p < 0.05, \*\*p < 0.01, \*\*\*p < 0.001. <sup>a</sup>TA 3 versus 12 month, <sup>b</sup>gastrocnemius 3 versus 12 month, <sup>c</sup>EDL 3 versus 12 month, <sup>d</sup>soleus 3 versus 12 month, <sup>e</sup>.

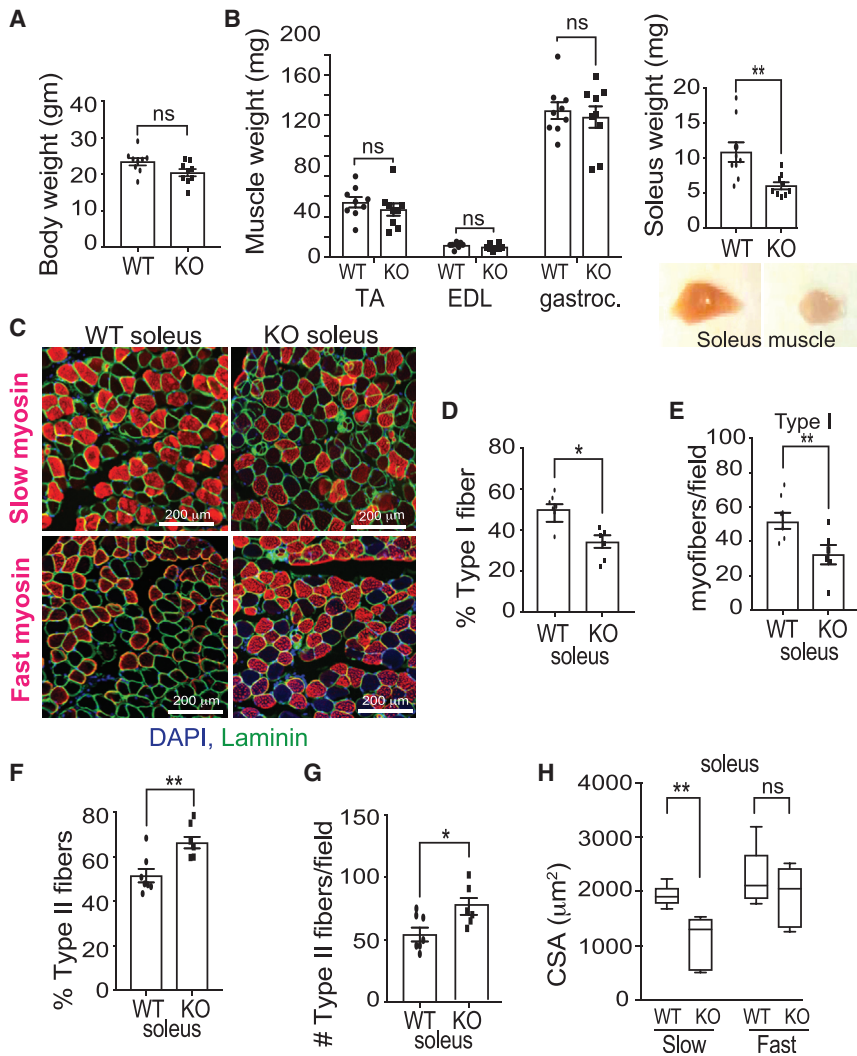


**Figure 5. Loss of AUF1 expression induces atrophy of slow-twitch myofibers**

(A) Body weight of WT and AUF1 KO mice at 3 months. (B) TA, gastrocnemius, EDL, and soleus muscle mass in 3-month-old WT and AUF1 KO mice. Representative image of WT and AUF1 KO soleus muscles shown. (C) Representative immunostain of slow (top) or fast (bottom) myosin (red) and laminin (green) in the soleus muscle from 3-month-old WT and AUF1 KO mice. Scale bars, 200  $\mu$ m. (D and E) Slow-twitch myofibers per field of percentage and number, respectively in 3-month-old WT and AUF1 KO mice. (F and G) Fast-twitch myofibers per field of percentage and number, respectively in 3-month-old WT and AUF1 KO mice. (H) Mean soleus slow- and fast-twitch myofiber CSA in 3-month-old WT and AUF1 KO mice,  $n = 6$  or 7 mice. Mean shown from 3 or more independent studies. \*  $p < 0.05$ , \*\*  $p < 0.01$  by unpaired Mann-Whitney U test.

can also interact with HuR, although the potential functional consequence is unknown, and AUF1 can also compete for binding to AREs with the AU-binding protein TIA-1, which blocks AUF1-mediated mRNA decay and ARE-mRNA translation.<sup>71</sup> Clearly, the role of ARE-binding proteins in myogenesis is complex and further investigation into their combined activities is needed to better understand this sophisticated regulation. How muscle homeostasis is regulated by AUF1 with the other ARE-binding proteins remains to be discovered.

Finally, it is important to note that although AUF1 specifies type I slow-twitch myofiber development, it also promotes and reprograms

the overall myogenesis program,<sup>46</sup> evidenced by the fact that AUF1 skeletal muscle gene transfer did not result in abnormal muscle development, abnormal balance of muscle fiber types, or muscle overgrowth.

## MATERIALS AND METHODS

### Mice

All animal studies were approved by the NYU School of Medicine Institutional Animal Care and Use Committee (IACUC) and conducted in accordance with IACUC guidelines. All *auf*<sup>-/-</sup> KO mice and WT mice are of the 129/B6-background, bred at the F3 and F4 generations from *auf*<sup>+/-</sup> heterozygous<sup>47,72</sup> 12-month-old C57BL/6 mice (Jackson) for AUF1 supplementation during AAV experiments.

### Cells

C2C12 cells were obtained from the American Type Culture Collection (ATCC), authenticated by STR profiling, and routinely checked

in turn likely further stimulate AUF1 expression as a result of exercise itself. Moreover, the effects of AUF1 gene transfer appear to be long-lasting. Improved exercise endurance in our study was found to be sustained for at least 6 months beyond the time of gene transfer, even in 18 and 24 month old mice (the last time point tested), with no evidence for reduction in AUF1 expression or efficacy. In this regard, AUF1 supplementation also increased levels of Pax7<sup>+</sup>-activated satellite cells and myoblasts, suggesting gene transfer into muscle stem cells and an active myogenesis process.

Apart from AUF1, other ARE RNA-binding proteins have also been shown to be involved in the myogenesis process. Of particular relevance to our study, HuR was recently found to destabilize *pgc1 $\alpha$*  mRNA, leading to the formation of type II myofibers.<sup>70</sup> It is noteworthy that AUF1 and HuR often have opposite effects on ARE-mRNA stability, in accord with our findings, and both are essential for the maintenance of myofiber specification. AUF1

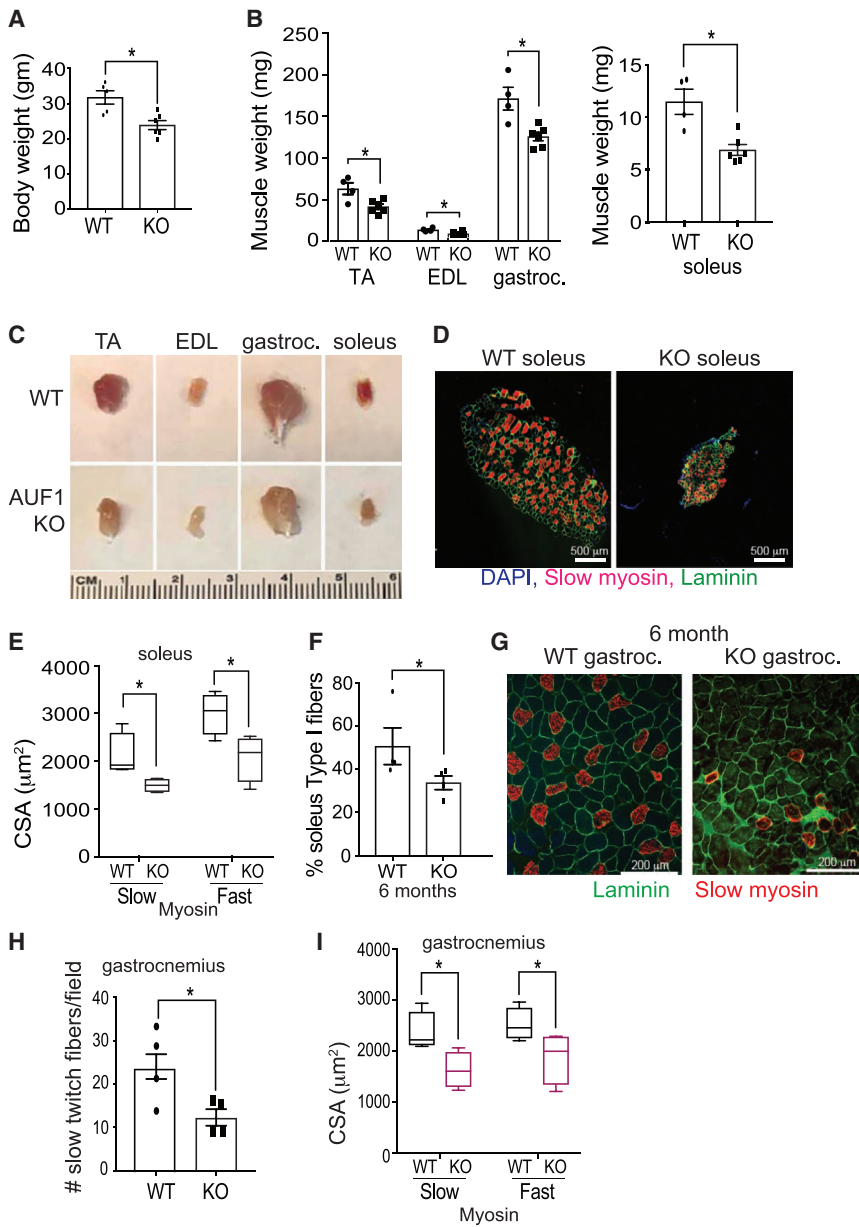


**Figure 6. AUF1 deletion induces slow- and fast-twitch muscle atrophy at 6 months of age**

(A) Body weight of WT and AUF1 KO mice at 6 months, n = 5 or 6 mice. (B) TA, EDL, gastrocnemius, and soleus muscle weight in 6-month-old WT and AUF1 KO mice. (C) Representative images of excised muscles from 6-month-old WT and AUF1 KO mice. (D) Representative immunostain of slow myosin (red) and laminin (green) in soleus muscle from 6-month-old WT and AUF1 KO mice. Scale bars, 500  $\mu\text{m}$ . (E) Mean CSA of slow- and fast-twitch myofibers in soleus muscle of 6-month-old WT and AUF1 KO mice. (F) Percentage of slow-twitch myofibers in 6-month-old WT and AUF1 KO mice in soleus muscle. (G) Representative staining of slow myosin (red) and laminin (green) in 6-month-old WT and AUF1 KO gastrocnemius muscle. Scale bars, 200  $\mu\text{m}$ . (H) Number of slow-twitch myofibers per field in gastrocnemius muscle of 6-month-old WT and AUF1 KO mice, n = 4 mice per group. (I) Mean gastrocnemius myofiber CSA of slow- and fast-twitch myofibers in 6-month-old WT and AUF1 KO mice, n = 4 mice per group. Mean  $\pm$  SEM from 4 or more independent studies. \*p < 0.05, \*\*p < 0.01 by unpaired Mann-Whitney U test.

**Immunofluorescence**

Mouse skeletal muscles were removed as indicated in Results, put in OCT, frozen in dry ice-cooled isopentane (Tissue-Tek), fixed in 4% paraformaldehyde, and blocked in 3% BSA in Tris-buffered saline (TBS). C2C12 cells were fixed in 4% paraformaldehyde and blocked in 3% BSA in PBS. Samples were immunostained overnight with antibodies: AUF1 (07-260, Millipore), Slow myosin (NOQ7.5.4D, Sigma), Fast myosin (MY-32, Sigma), Laminin alpha 2 (4H8-2, Sigma), GFP (2956, Cell Signaling), and Myf5 (clone AF 4027; R&D Systems). Anti myosin type I (BA-D5), IIa (SC-71, and IIb (BF-F3) were from Developmental Studies Hybridoma Bank. Slow and Fast myosin staining was done with the MOM Kit (Vector Labs). Alexa Fluor donkey 488, 555, anti-mouse IgG2b 594 (type I), anti-mouse IgG1 488 (IIa), and anti-mouse IgM 647 (IIb) were from

Thermo Fisher Scientific. Secondary antibodies were used at 1:300 and incubated for 1 h at room temperature. Slides were sealed with Vectashield with DAPI (Vector).

**Cloning and reporter assays**

The 3' UTR ARE region of mouse *PGC1a* was cloned into the vector pIS1 downstream of the *Renilla* luciferase cDNA with an EcoRV site. The pIS1-PGC1a-3' UTR or pIS1 control plasmids were transfected with TransIT-LT1 (Mirus Bio) into WT and WT AUF1-overexpressing C2C12 myoblasts. Cells were lysed after 24 h, and luciferase activity was measured with a dual-luciferase assay kit (Promega). All studies were performed in triplicate.

for mycoplasma contamination. C2C12 cells were maintained in DMEM (Corning), 10% fetal bovine serum (FBS) (GIBCO), and 1% penicillin-streptomycin (Life Technologies). To differentiate cells, medium was switched to DMEM (Corning), 2% horse serum (GIBCO), and 1% penicillin-streptomycin (Life Technologies) for 96 h.<sup>65</sup> *auf1* KO C2C12 cells were created with CRISPR-Cas9 methods.<sup>46</sup> For assays performed in the presence of actinomycin D to determine mRNA stability, C2C12 myoblast cells were treated with 0.2  $\mu\text{g}/\text{mL}$  of actinomycin D (Sigma). RNA immunoprecipitation experiments were done in WT C2C12 before and at 48 h of differentiation with a normal IgG rabbit control or a rabbit-anti AUF1 antibody (07-260, Millipore).

### Succinate dehydrogenase activity staining

Histochemical SDH staining was used as an index of muscle fiber oxidative capacity as described in [Results](#). Briefly, tissue sections were incubated in SDH incubation solution (sodium succinate 50 mM, nitroblue tetrazolium 0.5 mg/mL, and phosphate buffer 50 mM) for 1 h at 37°C. Tissue sections were washed in distilled water and mounted with glycerol-based mounting medium. Five fields chosen at random were quantified with ImageJ software.

### Microscopy and image processing and analysis

Images were acquired with a Zeiss LSM 700 confocal microscope, primarily with the 20× lens. Images were processed with ImageJ. If needed, color balance was adjusted linearly for the entire image and all images in experimental sets.

### Immunoblot studies

C2C12 cells or muscle tissues were lysed with lysis buffer (50 mmol/L Tris-HCl, pH 7.5, 150 mmol/L NaCl, 1 mmol/L EDTA, 1 mmol/L EGTA, 1% Triton X-100) supplemented with complete protease inhibitor cocktail (cOmplete Mini, Roche). Equal amounts of total protein were loaded on a polyacrylamide gel, resolved, and transferred to polyvinylidene fluoride (PVDF) membrane. Membrane was blocked with 5% nonfat milk in TBS-Tween 20 (0.1%) for 1 h and probed with antibody against AUF1 (07-260, Millipore), PGC1 $\alpha$  (Novus Biologicals NBP1-04676), and MEF2C (Cell Signaling D80C1). Bands were detected by peroxidase-conjugated secondary antibodies (GE Healthcare) and visualized with the ECL chemiluminescence system. The immunoblots were also probed with a rabbit antibody to  $\beta$ -tubulin (Cell Signaling 2146S) or GAPDH (Cell Signaling 2118S) as a control for loading. Quantification was performed by ImageJ.

### Real-time PCR analysis

RNA was extracted with TRIzol (Invitrogen) according to the manufacturer's instructions. DNase treatment was systematically performed. Quantification of extracted RNA was assessed with NanoDrop. The cDNA was synthesized with the High Capacity cDNA Reverse Transcription Kit (Applied Biosystems). mRNA was analyzed by real-time PCR using the iTaq Universal SYBR Green Supermix (Bio-Rad) probe. Relative quantification was determined by the comparative CT method with data normalized to housekeeping gene and calibrated to the average of control groups.

### AAV-AUF1 expression

AUF1 was integrated into an AAV8 under the tMCK promoter (AAV8-tMCK-AUF1-IRES-eGFP) (Vector Biolabs). We used AAV8-tMCK-IRES-eGFP as a control vector. This promoter was generated by the addition of a triple tandem of 2RS5 enhancer sequences (3-Ebox) ligated to the truncated regulation region of the muscle creatine kinase (MCK) promoter, which induced high muscle specificity.<sup>51</sup> C57BL/6 mice were injected with a single retro-orbital injection of 50  $\mu$ L (final concentration:  $2.5 \times 10^{11}$  genome copies). We performed muscle function tests (grid hanging time, time and dis-

tance to exhaustion, and maximum speed on a treadmill) 40 days or 6 months post injection. Mice were then euthanized, and tissues were collected.

### Muscle function tests

Muscle function tests were carried out as described previously.<sup>73</sup>

### Grid hanging time

Mice were placed in the center of a grid, 30 cm above soft bedding to prevent injury. The grid was then inverted. Grid hanging time was measured as the amount of time mice held on before dropping off the grid. Each mouse was analyzed twice, with 5 repetitions per mouse, with several hours of resting time between repetitions.

### Time, distance to exhaustion, and maximum speed

After 1 week of acclimation after tests, mice were placed on a treadmill and the speed was increased by 1 m/min every 3 min and the slope increased every 9 min by 5 cm to a maximum of 15 cm. Mice were considered to be exhausted when they stayed on the electric grid >10 s. Each mouse was analyzed twice, with 5 repetitions per mouse. Based on their weight and running performance, work performance was calculated in joules (J) as described previously<sup>73</sup> with the formula

$$\text{Work(J)} = \text{body weight(kg)} \times \text{running speed(m / s)} \times \\ \text{treadmill incline(angle)} \times \text{gravity(9.81m / s}^2\text{)}$$

### Quantification and statistical analysis

All results are expressed as means  $\pm$  SEM. Two-group comparisons were analyzed by the unpaired Mann-Whitney test. Multiple-group comparisons were performed with one-way analysis of variance (ANOVA). The non-parametric Kruskal-Wallis test followed by the Dunn's comparison of pairs was used to analyze groups when suitable. p values of <0.05 were considered significant. All statistical analyses were performed with GraphPad Prism (version 7) software. Muscle fiber number quantification involved no fewer than 5 fields per data point chosen at random and a minimum of 100 fibers per data point scored.

### SUPPLEMENTAL INFORMATION

Supplemental information can be found online at <https://doi.org/10.1016/j.omtm.2021.07.005>.

### ACKNOWLEDGMENTS

We thank Dr. William Coetzee of NYU School of Medicine for assistance in treadmill studies and the NYU Histopathology core for muscle sectioning. This work was supported by NIH Grant 1R01 AR074430-01 (R.J.S.), UL1 TR00038 from the National Center for Advancing Translational Sciences (NCATS) for core services support, and the Vilcek Postdoctoral Fellowship (D.A.).

### AUTHOR CONTRIBUTIONS

D.A. and R.J.S. designed the experiments. D.A. and J.J.A. carried out all studies. D.A. and O.K. performed PGC1 $\alpha$ -3' UTR molecular

cloning and luciferase assay experiments. D.A. and R.J.S. wrote the manuscript and analyzed and interpreted the data.

## DECLARATION OF INTERESTS

The authors declare no competing interests.

## REFERENCES

- Vermeiren, S., Vella-Azzopardi, R., Beckwee, D., Habbig, A.K., Scafoglieri, A., Jansen, B., and Bautmans, I.; Gerontopole Brussels Study Group (2016). Frailty and the Prediction of Negative Health Outcomes: A Meta-Analysis. *J. Am. Med. Dir. Assoc.* *17*, 1163.e1–1163.e17, 27886869.
- Buford, T.W. (2017). Sarcopenia: Relocating the Forest among the Trees. *Toxicol. Pathol.* *45*, 957–960.
- Short, K.R., Bigelow, M.L., Kahl, J., Singh, R., Coenen-Schimke, J., Raghavakaimal, S., and Nair, K.S. (2005). Decline in skeletal muscle mitochondrial function with aging in humans. *Proc. Natl. Acad. Sci. USA* *102*, 5618–5623.
- Cederholm, T., and Morley, J.E. (2015). Sarcopenia: the new definitions. *Curr. Opin. Clin. Nutr. Metab. Care* *18*, 1–4.
- Del Campo, A., Contreras-Hernández, I., Castro-Septúlveda, M., Campos, C.A., Figueroa, R., Tevy, M.F., Eisner, V., Casas, M., and Jaimovich, E. (2018). Muscle function decline and mitochondria changes in middle age precede sarcopenia in mice. *Aging (Albany NY)* *10*, 34–55.
- Wilkinson, D.J., Piasecki, M., and Atherton, P.J. (2018). The age-related loss of skeletal muscle mass and function: Measurement and physiology of muscle fibre atrophy and muscle fibre loss in humans. *Ageing Res. Rev.* *47*, 123–132.
- Feige, P., Brun, C.E., Ritso, M., and Rudnicki, M.A. (2018). Orienting Muscle Stem Cells for Regeneration in Homeostasis, Aging, and Disease. *Cell Stem Cell* *23*, 653–664.
- Feige, P., and Rudnicki, M.A. (2018). Muscle stem cells. *Curr. Biol.* *28*, R589–R590.
- Carlson, M.E., and Conboy, I.M. (2007). Loss of stem cell regenerative capacity within aged niches. *Aging Cell* *6*, 371–382.
- Schiaffino, S., and Reggiani, C. (2011). Fiber types in mammalian skeletal muscles. *Physiol. Rev.* *91*, 1447–1531.
- Hindi, S.M., Tajrishi, M.M., and Kumar, A. (2013). Signaling mechanisms in mammalian myoblast fusion. *Sci. Signal.* *6*, re2.
- Hernández-Hernández, J.M., García-González, E.G., Brun, C.E., and Rudnicki, M.A. (2017). The myogenic regulatory factors, determinants of muscle development, cell identity and regeneration. *Semin. Cell Dev. Biol.* *72*, 10–18.
- Buckingham, M., and Relaix, F. (2007). The role of Pax genes in the development of tissues and organs: Pax3 and Pax7 regulate muscle progenitor cell functions. *Annu. Rev. Cell Dev. Biol.* *23*, 645–673.
- Yin, H., Price, F., and Rudnicki, M.A. (2013). Satellite cells and the muscle stem cell niche. *Physiol. Rev.* *93*, 23–67.
- Seale, P., Sabourin, L.A., Girgis-Gabardo, A., Mansouri, A., Gruss, P., and Rudnicki, M.A. (2000). Pax7 is required for the specification of myogenic satellite cells. *Cell* *102*, 777–786.
- Lepper, C., Conway, S.J., and Fan, C.M. (2009). Adult satellite cells and embryonic muscle progenitors have distinct genetic requirements. *Nature* *460*, 627–631.
- von Maltzahn, J., Jones, A.E., Parks, R.J., and Rudnicki, M.A. (2013). Pax7 is critical for the normal function of satellite cells in adult skeletal muscle. *Proc. Natl. Acad. Sci. USA* *110*, 16474–16479.
- Price, F.D., von Maltzahn, J., Bentzinger, C.F., Dumont, N.A., Yin, H., Chang, N.C., Wilson, D.H., Frenette, J., and Rudnicki, M.A. (2014). Inhibition of JAK-STAT signaling stimulates adult satellite cell function. *Nat. Med.* *20*, 1174–1181.
- Hwang, A.B., and Brack, A.S. (2018). Muscle Stem Cells and Aging. *Curr. Top. Dev. Biol.* *126*, 299–322.
- Bassel-Duby, R., and Olson, E.N. (2006). Signaling pathways in skeletal muscle remodeling. *Annu. Rev. Biochem.* *75*, 19–37.
- Wang, Y., and Pessin, J.E. (2013). Mechanisms for fiber-type specificity of skeletal muscle atrophy. *Curr. Opin. Clin. Nutr. Metab. Care* *16*, 243–250.
- Tonkin, J., Villarroya, F., Puri, P.L., and Vinciguerra, M. (2012). SIRT1 signaling as potential modulator of skeletal muscle diseases. *Curr. Opin. Pharmacol.* *12*, 372–376.
- Arany, Z. (2008). PGC-1 coactivators and skeletal muscle adaptations in health and disease. *Curr. Opin. Genet. Dev.* *18*, 426–434.
- Nilwik, R., Snijders, T., Leenders, M., Groen, B.B., van Kranenburg, J., Verdijk, L.B., and van Loon, L.J. (2013). The decline in skeletal muscle mass with aging is mainly attributed to a reduction in type II muscle fiber size. *Exp. Gerontol.* *48*, 492–498.
- Proctor, D.N., Sinning, W.E., Walro, J.M., Sieck, G.C., and Lemon, P.W. (1995). Oxidative capacity of human muscle fiber types: effects of age and training status. *J. Appl. Physiol.* (1985) *78*, 2033–2038, 7665396.
- Sayed, R.K., de Leonardi, E.C., Guerrero-Martínez, J.A., Rahim, I., Mokhtar, D.M., Saleh, A.M., Abdalla, K.E., Pozo, M.J., Escames, G., López, L.C., and Acuña-Castroviejo, D. (2016). Identification of morphological markers of sarcopenia at early stage of aging in skeletal muscle of mice. *Exp. Gerontol.* *83*, 22–30.
- Verdijk, L.B., Koopman, R., Schaart, G., Meijer, K., Savelberg, H.H., and van Loon, L.J. (2007). Satellite cell content is specifically reduced in type II skeletal muscle fibers in the elderly. *Am. J. Physiol. Endocrinol. Metab.* *292*, E151–E157.
- Kadoguchi, T., Shimada, K., Miyazaki, T., Kitamura, K., Kunimoto, M., Aikawa, T., Sugita, Y., Ouchi, S., Shiozawa, T., Yokoyama-Nishitani, M., et al. (2020). Promotion of oxidative stress is associated with mitochondrial dysfunction and muscle atrophy in aging mice. *Geriatr. Gerontol. Int.* *20*, 78–84.
- Lin, J., Wu, H., Tarr, P.T., Zhang, C.Y., Wu, Z., Boss, O., Michael, L.F., Puigserver, P., Isotani, E., Olson, E.N., et al. (2002). Transcriptional co-activator PGC-1 alpha drives the formation of slow-twitch muscle fibres. *Nature* *418*, 797–801.
- Lai, R.Y., Ljubicic, V., D'souza, D., and Hood, D.A. (2010). Effect of chronic contractile activity on mRNA stability in skeletal muscle. *Am. J. Physiol. Cell Physiol.* *299*, C155–C163.
- Ekstrand, M.I., Falkenberg, M., Rantanen, A., Park, C.B., Gaspari, M., Hultenby, K., Rustin, P., Gustafsson, C.M., and Larsson, N.G. (2004). Mitochondrial transcription factor A regulates mtDNA copy number in mammals. *Hum. Mol. Genet.* *13*, 935–944.
- Scarpulla, R.C. (2008). Transcriptional paradigms in mammalian mitochondrial biogenesis and function. *Physiol. Rev.* *88*, 611–638.
- Wiggs, M.P. (2015). Can endurance exercise preconditioning prevent muscle atrophy? *Front. Physiol.* *6*, 63.
- Wing, S.S., Lecker, S.H., and Jagoe, R.T. (2011). Proteolysis in illness-associated skeletal muscle atrophy: from pathways to networks. *Crit. Rev. Clin. Lab. Sci.* *48*, 49–70.
- Bost, F., and Kaminski, L. (2019). The metabolic modulator PGC-1 $\alpha$  in cancer. *Am. J. Cancer Res.* *9*, 198–211.
- Dos Santos, J.M., Moreli, M.L., Tewari, S., and Benite-Ribeiro, S.A. (2015). The effect of exercise on skeletal muscle glucose uptake in type 2 diabetes: An epigenetic perspective. *Metabolism* *64*, 1619–1628.
- Robinson, D.C.L., and Dilworth, F.J. (2018). Epigenetic Regulation of Adult Myogenesis. *Curr. Top. Dev. Biol.* *126*, 235–284.
- Talbot, J., and Maves, L. (2016). Skeletal muscle fiber type: using insights from muscle developmental biology to dissect targets for susceptibility and resistance to muscle disease. *Wiley Interdiscip. Rev. Dev. Biol.* *5*, 518–534.
- Selsby, J.T., Morine, K.J., Pendrak, K., Barton, E.R., and Sweeney, H.L. (2012). Rescue of dystrophic skeletal muscle by PGC-1 $\alpha$  involves a fast to slow fiber type shift in the mdx mouse. *PLoS ONE* *7*, e30063.
- von Maltzahn, J., Renaud, J.M., Parise, G., and Rudnicki, M.A. (2012). Wnt7a treatment ameliorates muscular dystrophy. *Proc. Natl. Acad. Sci. USA* *109*, 20614–20619.
- Ljubicic, V., Burt, M., and Jasmin, B.J. (2014). The therapeutic potential of skeletal muscle plasticity in Duchenne muscular dystrophy: phenotypic modifiers as pharmacologic targets. *FASEB J.* *28*, 548–568.
- Moore, A.E., Chenette, D.M., Larkin, L.C., and Schneider, R.J. (2014). Physiological networks and disease functions of RNA-binding protein AUF1. *Wiley Interdiscip. Rev. RNA* *5*, 549–564.
- Chen, C.Y., and Shyu, A.B. (1995). AU-rich elements: characterization and importance in mRNA degradation. *Trends Biochem. Sci.* *20*, 465–470.

44. Kim, M.Y., Hur, J., and Jeong, S. (2009). Emerging roles of RNA and RNA-binding protein network in cancer cells. *BMB Rep.* *42*, 125–130.
45. Chenette, D.M., Cadwallader, A.B., Antwine, T.L., Larkin, L.C., Wang, J., Olwin, B.B., and Schneider, R.J. (2016). Targeted mRNA Decay by RNA Binding Protein AUF1 Regulates Adult Muscle Stem Cell Fate, Promoting Skeletal Muscle Integrity. *Cell Rep.* *16*, 1379–1390.
46. Abbadi, D., Yang, M., Chenette, D.M., Andrews, J.J., and Schneider, R.J. (2019). Muscle development and regeneration controlled by AUF1-mediated stage-specific degradation of fate-determining checkpoint mRNAs. *Proc. Natl. Acad. Sci. USA* *116*, 11285–11290.
47. Pont, A.R., Sadri, N., Hsiao, S.J., Smith, S., and Schneider, R.J. (2012). mRNA decay factor AUF1 maintains normal aging, telomere maintenance, and suppression of senescence by activation of telomerase transcription. *Mol. Cell* *47*, 5–15.
48. Nakao, R., Yamamoto, S., Yasumoto, Y., Kadota, K., and Oishi, K. (2015). Impact of denervation-induced muscle atrophy on housekeeping gene expression in mice. *Muscle Nerve* *51*, 276–281.
49. Yüzbaşıoğlu, A., Onbaşilar, I., Kocaefe, C., and Özgüç, M. (2010). Assessment of housekeeping genes for use in normalization of real time PCR in skeletal muscle with chronic degenerative changes. *Exp. Mol. Pathol.* *88*, 326–329.
50. Zhao, J., Tian, Z., Kadomatsu, T., Xie, P., Miyata, K., Sugizaki, T., Endo, M., Zhu, S., Fan, H., Horiguchi, H., et al. (2018). Age-dependent increase in angiotensin-like protein 2 accelerates skeletal muscle loss in mice. *J. Biol. Chem.* *293*, 1596–1609.
51. Wang, B., Li, J., Fu, F.H., Chen, C., Zhu, X., Zhou, L., Jiang, X., and Xiao, X. (2008). Construction and analysis of compact muscle-specific promoters for AAV vectors. *Gene Ther.* *15*, 1489–1499.
52. Brummer, H., Zhang, M.Y., Piddoubny, M., and Medler, S. (2013). Hybrid fibers transform into distinct fiber types in maturing mouse muscles. *Cells Tissues Organs* *198*, 227–236.
53. Augusto, V., Eduardo, G., Padovani, C.R., and Campos, R. (2004). Skeletal muscle fiber types in C57BL/6J mice. *J. Morphol. Sci.* *21*, 89–94.
54. Rao, V.V., and Mohanty, A. (2019). Immunohistochemical Identification of Muscle Fiber Types in Mice *Tibialis Anterior* Sections. *Bio Protoc.* *9*, e3400.
55. Matsuura, T., Li, Y., Giacobino, J.P., Fu, F.H., and Huard, J. (2007). Skeletal muscle fiber type conversion during the repair of mouse soleus: potential implications for muscle healing after injury. *J. Orthop. Res.* *25*, 1534–1540.
56. Paul, A.C., and Rosenthal, N. (2002). Different modes of hypertrophy in skeletal muscle fibers. *J. Cell Biol.* *156*, 751–760.
57. Sabourin, L.A., and Rudnicki, M.A. (2000). The molecular regulation of myogenesis. *Clin. Genet.* *57*, 16–25.
58. Riaz, M., Raz, Y., Moloney, E.B., van Putten, M., Krom, Y.D., van der Maarel, S.M., Verhaagen, J., and Raz, V. (2015). Differential myofiber-type transduction preference of adeno-associated virus serotypes 6 and 9. *Skelet. Muscle* *5*, 37.
59. Bezawork-Geleta, A., Rohlena, J., Dong, L., Pacak, K., and Neuzil, J. (2017). Mitochondrial Complex II: At the Crossroads. *Trends Biochem. Sci.* *42*, 312–325.
60. Cartee, G.D., Hepple, R.T., Bamman, M.M., and Zierath, J.R. (2016). Exercise Promotes Healthy Aging of Skeletal Muscle. *Cell Metab.* *23*, 1034–1047.
61. Yoo, S.Z., No, M.H., Heo, J.W., Park, D.H., Kang, J.H., Kim, S.H., and Kwak, H.B. (2018). Role of exercise in age-related sarcopenia. *J. Exerc. Rehabil.* *14*, 551–558.
62. Potthoff, M.J., and Olson, E.N. (2007). MEF2: a central regulator of diverse developmental programs. *Development* *134*, 4131–4140.
63. Potthoff, M.J., Olson, E.N., and Bassel-Duby, R. (2007). Skeletal muscle remodeling. *Curr. Opin. Rheumatol.* *19*, 542–549.
64. Potthoff, M.J., Wu, H., Arnold, M.A., Shelton, J.M., Backs, J., McAnally, J., Richardson, J.A., Bassel-Duby, R., and Olson, E.N. (2007). Histone deacetylase degradation and MEF2 activation promote the formation of slow-twitch myofibers. *J. Clin. Invest.* *117*, 2459–2467.
65. Panda, A.C., Abdelmohsen, K., Yoon, J.H., Martindale, J.L., Yang, X., Curtis, J., Mercken, E.M., Chenette, D.M., Zhang, Y., Schneider, R.J., et al. (2014). RNA-binding protein AUF1 promotes myogenesis by regulating MEF2C expression levels. *Mol. Cell. Biol.* *34*, 3106–3119.
66. Masuda, K., Marasa, B., Martindale, J.L., Halushka, M.K., and Gorospe, M. (2009). Tissue- and age-dependent expression of RNA-binding proteins that influence mRNA turnover and translation. *Aging (Albany NY)* *1*, 681–698.
67. Matravadia, S., Martino, V.B., Sinclair, D., Mutch, D.M., and Holloway, G.P. (2013). Exercise training increases the expression and nuclear localization of mRNA destabilizing proteins in skeletal muscle. *Am. J. Physiol. Regul. Integr. Comp. Physiol.* *305*, R822–R831.
68. D'souza, D., Lai, R.Y., Shuen, M., and Hood, D.A. (2012). mRNA stability as a function of striated muscle oxidative capacity. *Am. J. Physiol. Regul. Integr. Comp. Physiol.* *303*, R408–R417.
69. Haralampieva, D., Salemi, S., Dinulovic, I., Sulser, T., Ametamey, S.M., Handschin, C., and Eberli, D. (2017). Human Muscle Precursor Cells Overexpressing PGC-1 $\alpha$  Enhance Early Skeletal Muscle Tissue Formation. *Cell Transplant.* *26*, 1103–1114.
70. Janice Sánchez, B., Tremblay, A.K., Leduc-Gaudet, J.P., Hall, D.T., Kovacs, E., Ma, J.F., Mubaid, S., Hallauer, P.L., Phillips, B.L., Vest, K.E., et al. (2019). Depletion of HuR in murine skeletal muscle enhances exercise endurance and prevents cancer-induced muscle atrophy. *Nat. Commun.* *10*, 4171.
71. Pullmann, R., Jr., Kim, H.H., Abdelmohsen, K., Lal, A., Martindale, J.L., Yang, X., and Gorospe, M. (2007). Analysis of turnover and translation regulatory RNA-binding protein expression through binding to cognate mRNAs. *Mol. Cell. Biol.* *27*, 6265–6278.
72. Lu, J.Y., Sadri, N., and Schneider, R.J. (2006). Endotoxic shock in AUF1 knockout mice mediated by failure to degrade proinflammatory cytokine mRNAs. *Genes Dev.* *20*, 3174–3184.
73. Castro, B., and Kuang, S. (2017). Evaluation of Muscle Performance in Mice by Treadmill Exhaustion Test and Whole-limb Grip Strength Assay. *Bio Protoc* *7*, e2237, 28713848.